Cyclodextrin-based nanosponge for improvement of solubility and oral bioavailability of Ellagic acid

Fatma Mohammed Mady[1,2]* and Sabrin Ragab Mohamed Ibrahim[3]

[1]Department of Pharmaceutics & Pharmaceutical Technology, Faculty of Pharmacy, Taibah University, Medina, Saudi Arabia
[2]Department of Pharmaceutics, Faculty of Pharmacy, Minia University, Minia, Egypt
[3]Department of Pharmacognosy and Pharmaceutical Chemistry, Faculty of Pharmacy, Taibah University, Medina, Saudi Arabia

Abstract: Ellagic acid (EA) is a polyphenolic compound, naturally occurring in various fruits. It has antioxidant, anticancer and antimutagenic properties. Its low aqueous solubility and permeability in GIT, permanent binding to DNA and proteins of cells and first pass metabolism are considered as the reasons for its low oral bioavailability and consequently its low therapeutic potential. Cyclodextrin-based nanosponges (NS) have been utilized to improve the solubilization efficiency of Ellagic acid and to control its release. The scope of the work was to prepare EA nanosponges (EA-NS) using cyclodextrin (β-CD) and cross-linked by dimethyl carbonate (DMC). It was found that the particle size of the prepared EA-NS was 423.2 nm with low polydispersity index (0.409) and high zeta potential (-34 mV) which manifests the construction of a stabilized colloidal nanoformulation. Moreover, high solubilization efficiency of the loaded EA-NS (49.79µg/ml) compared with the free EA (9.73µg/ml) was spotted. The prepared EA-NS was characterized by XRD, FTIR, and DSC studies and it elucidated a definite interaction of EA with NS. EA-NS successively improved its solubility and provided a controlled in vitro release for 24 hours. EA-NS produced about 69.17 % drug content which indicates a good drug loading of the prepared nanosponges. Dissolution of EA-NS was higher than the drug alone. Animal study displayed an improvement in the oral bioavailability of EA indicated by an increase in AUC (1345.49 ng.hr.ml^{-1}) of the EA -NS compared with (598.94 ng.hr.ml^{-1}) for EA.

Keywords: Ellagic acid, nanosponge, β-cyclodextrin, oral bioavailability.

INTRODUCTION

Acide ellagique, as discovered by the chemist Henri Braconnot (Labrude and Becq 2003), is a natural polyphenol extracted from many kinds of fruits such as berries, pomegranates, walnut and various vegetables (Vattem and Shetty 2005, Zhang *et al*., 2014). Ellagic acid (EA) occurs as a free moiety, as glycosylated and/or acylated derivative, or jointed with glucose as ellagitannins. It composes of four aromatic rings elucidating the hydrophobic part, with another four hydroxyl groups and a couple of lactone rings indicating the hydrophilic moiety (Aguilera-Carbo *et al*., 2008). Numerous researchers emphasized the usefulness of EA as an antioxidant, anti-inflammatory, antiapoptotic, antimutagenic, hepatoprotective, cardioprotective and for neurological disorders of diabetics (Anderson *et al*., 2001, Sharma *et al*., 2007). Although, EA has offered a great safety and efficacy profile, it didn't show a good therapeutic utilization owing to its low aqueous solubility and low oral bioavailability (Byrne *et al*., 2008, Lei *et al*., 2003). Furthermore, opening of the lactone ring of EA by the intestinal flora will lead to its rapid elimination from the body and short half-life (Bulani *et al*., 2016). The diminished oral absorption of EA may be accredited to its limited solubility in water, gut metabolism (González-Sarrías *et al*., 2015, Seeram *et al*., 2004), extensive hepatic metabolizing effect and irreversible binding to cellular DNA and proteins. This requests techniques to enhance the oral bioavailability of EA. Nano-formulations of these poorly soluble drugs or their nanosizing, will lead to an improvement of the solubility and consequently the bioavailability. Various studies are involved in the advancement of novel approaches to increase the solubility of EA as well as to extend its release. Our potential method to enhance its clinical usefulness was to incorporate it within the internal core of a nanoparticles, which improved the dissolution as well as controlled the release rate of the drug (Mady and Shaker, 2017). Since nano-size particles are capable to transfer through the intestinal barrier in its intact form via the M-cells presented in the Peyer's patches through the intra-cellular endocytosis mechanism (Lopes *et al*., 2014). This endocytosis technique is encouraged primarily by the interaction between the nanoparticles and cells through nonspecific hydrogen bond and van der Waal attraction bonds (Florence 1997, Lopes *et al*., 2014). These invaginated nanoparticles transport to the systemic circulation through the lymphatic system. The suitability of nano-formulations enables them to enhance the bioavailability, decrease the desired dosage and ultimately enhance the efficiency of the incorporated drug due to the capability of off-setting the gut wall degradation enzymes and the first pass metabolism (Brayden *et al*., 2005, Clark *et al*., 2001, Florence, 1997, Lopes *et al*., 2014).

**Corresponding author:* e-mail: fatmamady@hotmail.com

Many studies stated that the inclusion complex formation of polyphenols with cyclodextrins improves their aqueous solubilities and consequently enhances their antioxidant effects (Cutrignelli *et al*., 2014, Ferreira *et al*., 2013).

Moreover, nanosponge is a novel technology which facilitated targeted delivery of drug for extended period of time for internal use. Nanosponge formation is an effective technique for the entrapment of various kinds of drugs and they can fulfill this through inclusion or non-inclusion complex formation (Mohanty and Sahoo 2010). The cyclodextrin-based nanosponges (CD-NS) are hyper cross-linked sponge-like, polymeric constructions, obtained from β- cyclodextrins with a great efficacy to interact with small drugs in its structure (Swaminathan *et al*., 2007). Recently, CD-NS are used as drug delivery systems to enhance the therapeutic efficiency and bioavailability of the poorly soluble molecules (Cavalli *et al*., 2006, Torne *et al*., 2010) The highly cross-linked construction of the CD-NS together with their CD cavities are cooperated to form inclusion complexes with drug molecules. In addition, the formed nanochannels in the polymer network are able to trap the guest drug molecules. This distinctive organizational structure favors the complexation of drugs and could be accountable for the enhanced solubility, stabilization and protective ability of NS compared with its original CDs. Colloidal nanosuspension is formed after the dispersion of drug-loaded NS in an aqueous medium with a sustained drug release profile (Swaminathan, Cavalli, *et al*., 2010). The suitability of cavity size of β-cyclodextrin (β-CD) made it more commonly used for the inclusion of various types of hydrophobic molecules.

The present study was aimed to estimate the effect of ellagic acid loaded-β-cyclodextrin nanosponge (EA-NS) on the solubility, dissolution and oral bioavailability of Ellagic acid (EA). The characterization of the prepared NS was performed by DSC, XRD, FTIR and SEM studies. In vitro dissolution studies were also performed and compared with the pure drug. In addition, *in vivo* pharmacokinetic study was carried out after oral administration of the prepared NS compared with the crude EA.

MATERIALS AND METHODS

Materials

β-Cyclodextrin, dimethyl formamide, triethyl amine and dimethyl carbonate were purchased from Sigma-Aldrich. All other chemicals are of analytical grade.

Methods

Isolation and characterization of ellagic acid

Pomegranate was obtained from a local market (Al-Madinah Al-Munawwarah, KSA). The plant was authorized by Dr. Nahed Morad, Faculty of Science, King Abdulaziz University. A specimen (PO-1-2016) was preserved at Pharmacognosy and Pharmaceutical Chemistry Department, College of Pharmacy, Taibah University. The powdered rinds (800 g) were extracted with 70% MeOH (3 L×4). The combined extract was concentrated under vacuum to get a dark brown residue (29.3 g). The later was subjected to acid hydrolysis using 10 % H_2SO_4 in MeOH with refluxing for 3 hr (Lu and Yuan, 2008). The hydrolysis product was concentrated and passed through sephadex LH-20, eluting with MeOH to get four fractions: PR-1: PR-4. By TLC monitoring, fraction PR-3 was chosen to separate ellagic acid. Fraction PR-3 was concentrated and repeatedly recrystallized from MeOH to afford impure ellagic acid. Subsequently, it was subjected to RP18 CC (100 g, 50 × 3 cm) using gradient of H_2O/MeOH to obtain ellagic acid. That was further identified by ^1H and ^{13}C NMR, UV, and EIMS experiments, in addition to comparing with formerly published data (Nawwar *et al*., 1994).

Spectral data

Brown residue; UV (MeOH) λ_{max}: 256, 368 nm; ^1H NMR (CD_3OD 500 MHz): δ_H 7.53 (H-4, 9); ^{13}C NMR (CD_3OD 125 MHz): δ_C 137.7 (C-1a, 6a), 141.0 (C-2, 7), 149.5 (C-3, 8), 111.7 (C-4, 9), 109.5 (C-4a, 9a), 114.2 (C-4b, 9b), 161.6 (C-5, 10); EIMS: m/z 302 $[M]^+$.

Hitachi-300 spectrophotometer was utilized to get UV spectrum. EIMS was acquired by mass spectrometer (JEOL JMS-SX/SX 102A). BRUKER Unity INOVA 500 was used for NMR spectra measurement (Bruker BioSpin, Billerica, MA, USA). SiO_2 60 F_{254} pre-coated plates (0.2 mm, Merck, Darmstadt, Germany) were used for TLC. Purification of compound was achieved using RP-18 and sephadex LH-20 (Merck, Darmstadt, Germany). The structure of ellagic acid was displayed in fig. 1.

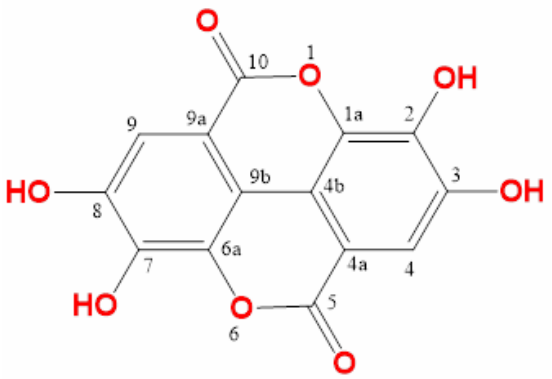

Fig. 1: Structure of Ellagic acid

Preparation of Ellagic-loaded nanosponges (EA-NS)

The preparation of CD-NS was performed using dimethyl carbonate as a cross-linker as previously reported (Darandale and Vavia, 2013, Shende *et al*., 2015). Shortly, 30ml of dimethyl formamide (DMF) was used to dissolve 2g of β-CD. Then 1ml of triethyl amine was added to the

formed CD solution. After that, 15ml of dimethyl carbonate was added, and the solution was sonicated for 10 min. Finally, the solvent was distilled out after refluxing the prepared solution for 4 h. The retained lump was the plain nanosponges. The formed mass of plain NS was washed with 25ml distilled water and 25 ml ethanol for purification. Finally drying of the plain NSs were carried out at 80°C and was exposed to soxhlet separation using 200 ml of ethanol for 24h.

Solubilization efficiency

Solubility of EA and EA-NS was determined as previously reported (Dora *et al*., 2016). Briefly, a sealed glass bottles containing excess of EA and EA-NS were added to water at ambient temperature. The bottles were agitated at 100 rpm overnight using shaking water bath, then centrifuged at 10,000 rpm for 5 min and filtered. The filtrate was suitably diluted and analyzed by UV spectrophotometer at max λ254

Characterization of the prepared EA-NS

Determination of size, polydispersity index and Zeta potential of nanosponges

NS sizes, polydispersity indices (PDI) and zeta potentials were measured using a zetasizer (Malvern, Ver. 6.01) at a fixed angle at 25°C. Nanosponges were suitably diluted with distilled water before it was analyzed.

Scanning electron microscopy (SEM)

Surface properties of the prepared NS was characterized by scanning electron microscopy (SEM) method for that scanning electron microscope (model LEO 435VP Cambridge, UK) was used with 15Kv accelerating voltage condition and different resolutions of the samples were taken.

Fourier transform infrared spectroscopy (FTIR)

It is used to examine the potential of interaction between drug and polymer. FTIR spectroscopic studies for crude EA, Empty NS and EA-NS were performed by formation of KBr disc using Shimadzu FT-IR 8400 spectrophotometer at a scanning speed between 4000- 400 cm^{-1}.

X-ray powder diffraction (XRPD)

Crude EA, plain NS and EA-NS were exposed to CuKα radiation (40 kV × 20mA) in the X-ray diffractometer (Siemens D5000, Munich, Germany) with a graphite monochromator. The scan was taken in the 2h range, 5–60° with a scanning speed and step size of 10/mm and 0.010, respectively.

Differential scanning calorimetry (DSC)

Thermograms were represented using (Perkin Elmer DSC, USA) instrument to estimate the thermal behavior of EA. The calibration of the device was carried out with indium for measuring of the fusion and melting point. A temperature range of heat 30-550◦C was adjusted using a heating rate of 10°C/min. Analyses were performed in triplicate on 5 mg of EA, empty NS, and EA-loaded NS separately under nitrogen purge and a flow rate of 20 ml/min.

Determination of Drug content

A weighed amount (5mg) of EA-loaded NS was suspended into water and sonicated for 30 min. After centrifugation at 5000 rpm for 5 min, the supernatant was analyzed using UV-Vis spectrophotometer (Hitachi-300 spectrophotometer) at λ_{max} at 254 after suitable dilution.

In vitro release of EA from nanosponges

The in vitro release studies were performed using dialysis membrane (Sartorius, cut off 12,000 Da). A fixed amount of EA-NS was suspended in 1 ml phosphate buffer at pH 6.8 and was placed in the donor portion. The receiving phase, which consisted of phosphate buffer pH 6.8 kept at 37±1°C, was completely removed and replaced with fresh medium after predetermined time intervals (0.5, 1, 2, 4, 8, 10, 12, 24 h). The removed solution was suitably diluted and analyzed by UV-Vis spectrophotometer at λ_{max} at 254 nm. The experiment was performed in triplicate.

Kinetic models of dissolution profiles of Ellagic acid-loaded nanosponges

Different mathematical functions are used to describe various which characterize the mechanism of release of EA from nanosponges. The dissolution mechanism is characterized based on the derived model parameters after a suitable model has been chosen (Dash *et al*., 2010).

In vivo pharmacokinetic study

Animals and dosing

Two groups with 6 male New Zealand white rabbits in each group weighing 2Kg each were housed under standard conditions in the Animal House, Pharmacology Department, Faculty of Medicine, Assiut University, Assiut, Egypt. The study was carried out under the ethical standard guideline given for animal care during research. All rabbits were kept with a free access to water all over the period of the experiment. A dose of 50 mg/ Kg of body weight of free EA suspension was orally administered to one group while an equivalent dose of EA-NS was given to the other group of rabbits. Plasma samples were collected from the blood samples by their centrifugation at 6000 rpm for 2min. All samples were stored at 4°C until used.

The EA concentration in plasma samples was determined using HPLC system and plasma extraction procedures as previously reported (Bala *et al*., 2006, Mady and Shaker 2017). Briefly, it was composed of K-500 solvent delivery pump, injector valve with a 20µl loop and K-2500 UV variable wave length detector. The HPLC system control and data processing were carried out by computer

integration software (Euro Chrom 2000®Knauer). GeminiRP-C_{18} column (150x4.6mm, 5µm), (phenomenex, USA) was utilized.

Procedure for plasma extraction

Five hundred µL of plasma were fitted to pH 2.5 using 150µL of 1mol/L potassium dihydrogen phosphate solution and 15µL 50% phosphoric acid. Each sample was vortexed with 2.5ml acetonitrile for 1 min and centrifuged at 3500g for 10min. The supernatant was evaporated to dryness under nitrogen. The residue was reconstituted in 50 µL of the mobile phase. A 20µL was injected into the HPLC system for determination of EA in plasma (Seeram *et al*., 2004). The mobile phase consisted of a mixture of acetonitrile: 30mM phosphate buffer (adjusted to pH 3.5 with ortho-phosphoric acid) in a ratio of 60:40, v/v. Then it was filtered through a 0.45 mm membrane filter (Phenomenex, USA) and was degassed in an ultrasonic cleaner (Cole-Parmer, Chicago, IL, USA) and delivered at flow rate 1 mL/min.

Pharmacokinetic data analysis

EA pharmacokinetic parameters were estimated by fitting the plasma level–time data to the suitable model using WinNonlin™ standard version 1.5 (Scientific Consulting, Apex, NC, USA) software. Goodness of fit was assessed by visual inspection of the fitted curve and correlation coefficient, which exceeded 0.95. Absorption half-life ($t_{1/2Ka}$), elimination half-life ($t_{1/2}$), the area under the plasma EA concentration versus time curve (AUC_{0-t}), the peak concentration (C_{max}) and time to reach the peak concentration (T_{max}) were calculated according to conventional algorithms.

RESULTS

Solubilization efficiency

The solubility of the nanosponge was higher than the crude EA. High solubilization efficiency of the loaded EA-NS (49.79µg/ml) compared with the free EA (9.73 µg/ml) was observed.

Particle size, polydispersity index and Zeta potential of nanosponges

The mean particle size of EA-NS was 423±31 nm with a low particle size distribution (PDI =0.409±0.05). The measured zeta potential of the nanosponge was −34.51 mV.

SEM

The nanosponges were roughly spherical in shape as shown in fig. 2 with different magnifications. On the surface of the nanosponge formulations there existed a few drug particles and many tiny channel pores. EA-nanosponges were more porous in nature compared with plain nanosponges.

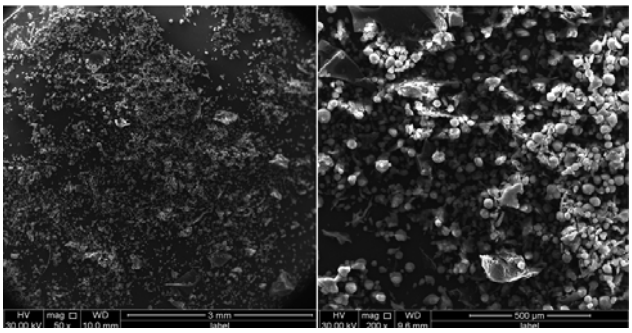

Fig. 2: EA-NS morphology using SEM with different magnifications.

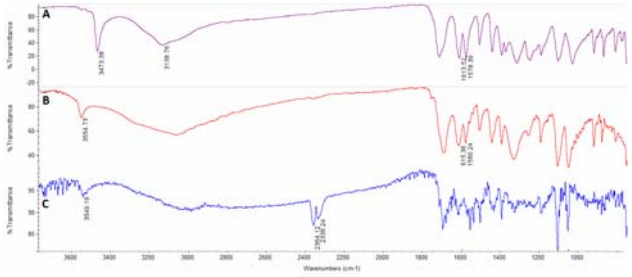

Fig. 3: FTIR spectral assignments of (A) EA, (B) empty NS and (C) EA-loaded NS.

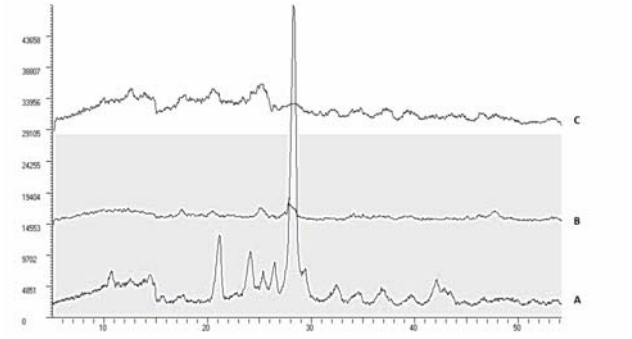

Fig. 4: X-ray diffractograms of (A) EA, (B) empty NS and (C) EA-loaded NS.

FTIR

The FTIR spectra of free EA, plain NS and EA-loaded NS are displayed in fig. 3. A sharp stretching band at 3473 cm^{-1} was observed which characterizes the phenolic OH group, while the stretching peak displayed at 1714cm^{-1} corresponds to C=O stretching. Absorption peak visualized in the area of 1320-1000cm^{-1} corresponding to ester linkage, while the aromatic ring vibrations were displayed at 1613 and 1578cm^{-1}. An olefinic C-H bending vibration, an aromatic C-O stretching vibration and C-O-C stretching vibrations of the EA were observed at 1427cm^{-1}, 1273cm^{-1} and 1026/856 cm^{-1}, respectively. The empty NS displayed a distinctive band at around 1720 cm^{-1} corresponding to the carbonate bond which emphasized the construction of CD-based NS. Moreover, the other characteristics peaks of NS were found at 1418 cm^{-1} due to C-H bending vibration and 1026 cm^{-1} due to C-O stretching vibration of primary alcohol. In FTIR spectral

assignments of EA-NS, all the characteristic bands related to the nanosponge were visualized and only few peculiar bands of EA are appeared. Due to the complex formation of EA with CD-NS, the bands belonging to the NS were observed at shifted wave-numbers, i.e., 3549cm^{-1}, 1418–1409cm^{-1} and 1056–1059 cm^{-1} which are corresponding to OH phenolic, C-H bending and C-O-C stretching vibrations, respectively. In addition, the appearance of new two characteristic bands at 2364-2338 cm^{-1} in FTIR spectra of EA-NS which were not present in the EA or the plain NS.

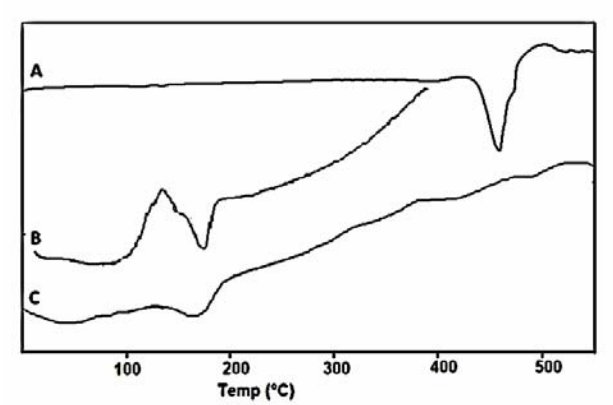

Fig. 5: DSC thermograms of (A) EA, (B) empty NS and (C) EA-loaded NS.

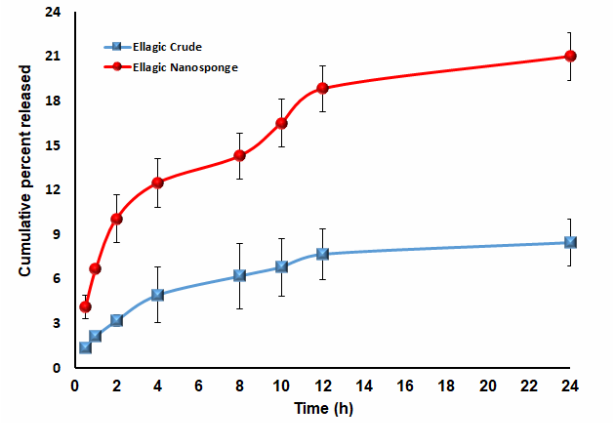

Fig. 6: *In vitro* release profile of EA from EA-loaded NS compared with the crude EA in phosphate buffer pH 6.8 at 37±1°C.

XRD

XRD is an insightful method to characterize the interaction between CyDs and guest molecules. XRD pattern of pure EA, empty NS and EA-loaded NS were investigated in order to study the physical properties and the crystallinity of EA within the CD-NS (fig. 4). Ellagic acid displayed a set of characteristic peaks at 10.41, 13.88, 21.69, 26.42, 27.81 and 31.32° suggesting its crystalline nature, while the diffractogram of the loaded NS exhibited the disappearance or weakening of some spectral lines of the drug such as 10.41, 27.81 and 31.32.

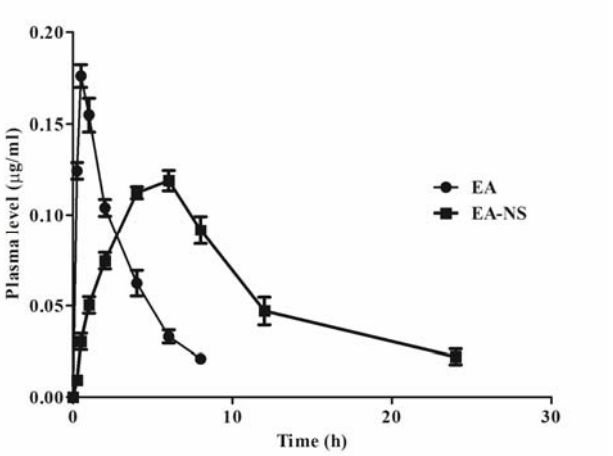

Fig. 7: Plasma concentration-time curve of EA and EA-NS after their oral administration to white rabbits.

DSC

Fig. 5 displays the DSC thermograms of pure EA, empty NS and EA-NS. The results displayed an endothermic peak at 460°C of the pure EA. This definite peak was disappeared in the EA-NS formulation.

Drug content in the prepared EA-NS

The % drug content of EA was determined in the prepared nanosponges and it was sufficiently promising value (69.17%).

In vitro release studies

Fig. 6 displayed the in vitro release study of EA from EA-NS compared with the crude drug. An initial rapid release was observed, thereafter, a prolonged release phase of the drug was spotted.

The release rate kinetics of the drug from the prepared NS which will indicate the mechanism of the drug release are shown in table 1. The obtained in-vitro drug release data was fitted to different mathematical models such as zero order, First order, Higuchi matrix, Hixon-crowel and Korsmeyer Peppas model. The regression coefficients (r) values ranged between 0.897 and 0.981.

In vivo study

Fig. 7 showed the plasma level- time curve which displayed a longer T_{max} (4.71h) and a lower C_{max} (110.45±0.005ng/ml) of EA-NS compared with those of the free drug (0.624 h and 166.1ng/ml).

Table 2 showed the pharmacokinetic parameters measured after oral administration of the prepared EA-NS compared with that of the crude drug. It showed an improvement in the oral bioavailability of EA indicated by an increase in AUC (1345.49 ng.hr.ml^{-1}) of the EA -NS compared with (598.94 ng.hr.ml^{-1}) for EA.

Table 1: Kinetic models of drug release from the prepared EA-NS

EA-NS	zero	First	Second	Diffusion	Hixon Crowel	Baker-Londsale	Korsemeyer peppas
a	7.8732	1.9645	0.01085	3.2621	0.12493	0.00101	-2.4617
b	0.0111	-5.6E-05	1.5E-06	0.5168	0.00019	5.62E-06	0.4105
r	0.897	-0.908	0.918	0.971	0.904	0.957196	0.981
k	0.0111	-0.0001	1.5E-06	0.517	0.0002	5.62E-06	0.00345
n	--	-	-	-	-	-	0.4105

a is slope
b is intercept
r is regression
K is a kinetic constant
n is the diffusional release exponent.

Table 2: Pharmacokinetic parameters of the EA after oral administration of 50 mg/kg of free and equivalent amount of EA-NS to rabbits (n= 6)

Pharmacokinetic parameter	Crude EA	EA-NS formulation
$AUC_{(0-t)}$ (ng.hr.ml^{-1})	598.94±44.62	1345.49±176.6
T_{max} (h)	0.649±0.061	4.558±0.38
C_{max} (ng/ml)	171.15±0.05	108.59±0.054
$ta_{1/2}$ (h)	0.169±0.025	3.159±0.147
$te_{1/2}$ (h)	1.918±0.23	3.16±0.16

AUC: Area under the plasma level time curve, C_{max}: the peak concentration, T_{max}: time to reach the peak concentration, $ta_{1/2}$: absorption half-life, $te_{1/2}$: elimination half-life.

DISCUSSION

The spotted solubility improvement might be attributed to the inclusion of the drug within the hydrophobic core in the nanosponge network and hence masking the hydrophobic functions of EA by NS (Swaminathan, Pastero *et al*., 2010).

A good stability of the prepared EA-NS after their dispersion in aqueous medium is indicated by the high zeta potential value (Kobayashi *et al*., 2014).

The more porous surface of nanosponges which observed in the SEM could be due to the incorporation of drug particles inside the nanosponge structure.

The characteristic peaks of EA were exhibited in its FTIR spectrum and it agreed with the previous reports (Puică *et al*., 2006). The FTIR data assure definite interactions between EA and NS in EA-NS formula.

A high crystallinity of pure EA was observed via its appeared definite peaks in XRD. The disappearance of such distinct peaks of EA in formulated EA-NS obviously elucidates that the incorporated EA in NSs is in the amorphous or in the solubilized solid state in the polymeric structure. The amorphous or the solubilized solid drug is readily diffusible through the polymeric matrix, controlling the release of the loaded drug (Mohanty and Sahoo 2010). The reduction of crystallinity may be an additive attribution to the enhancement of solubility of EA in the CD-NS along with the inclusion complexation.

The DSC results indicated a high thermal stability of EA. The absence of the definite melting peak of the drug in the EA-NS formulation referred to the complexation of EA in the prepared NS.

Drug content indicates an efficient entrapping of EA in the prepared EA-NS. The entrapping efficiency of nanosponges depends majorly on the degree of crystallization. Paracrystalline nanosponges may display different entrapping efficiencies (Swaminathan, Pastero *et al*., 2010).

An initial rapid release was observed, which is located in the matrix surface but not involved in the inclusion complex. Then, a prolonged release phase of the drug was spotted due to the presence of EA in the inclusion network.

The diffusional release exponent (n) is indicative of the operating release mechanism, and the calculated diffusion coefficient values ($n \leq 0.5$) were indicative of the fact that the drug release from the NS follows Case I transport; Fickian diffusion; Higuchi release mechanism (Dash *et al*., 2010).

The pharmacokinetic data showed an improvement in the oral bioavailability of EA indicated by an increase in AUC of the EA-NS compared with for EA. The longer

T_{max} and lower C_{max} indicate a sustained release effect of NS formulation of EA.

CONCLUSION

Nanosponge technique is a promising approach in controlling drug delivery systems. Improvement of aqueous solubility, dissolution and bioavailability of EA was implemented by the cyclodextrin nanosponge formulation. The higher solubility, the improved bioavailability and the controlled release of EA are attributed to the dual benefits of the presence of the drug in the nanocavities of the nanosponge and the inclusion phenomenon of the cyclodextrin. Therefore, this may result in a decrease in dosing value and dose dependent adverse effects and in the same time increase its therapeutic potential compared with the crude drug.

REFERENCES

Aguilera-Carbo A, Augur C, Prado-Barragan LA, Favela-Torres E and Aguilar CN (2008). Microbial production of ellagic acid and biodegradation of ellagitannins. *Appl. Microbiol. Biotechnol.,* **78**(2): 189-99.

Anderson KJ, Teuber SS, Gobeille A, Cremin P, Waterhouse AL and Steinberg FM (2001). Walnut polyphenolics inhibit in vitro human plasma and LDL oxidation. *J. Nutr.,* **131**(11): 2837-2842.

Bala I, Bhardwaj V, Hariharan S and Kumar MNVR (2006). Analytical methods for assay of ellagic acid and its solubility studies. *J. Pharm. Biomed. Anal.,* **40**(1): 206-210.

Brayden DJ, Jepson MA and Baird AW (2005). Keynote review: Intestinal Peyer's patch M cells and oral vaccine targeting. *Drug Discov. Today*, **10**(17): 1145-1157.

Bulani VD, Kothavade PS, Kundaikar HS, Gawali NB, Chowdhury AA, Degani MS and Juvekar AR (2016). Inclusion complex of ellagic acid with β-cyclodextrin: Characterization and *in vitro* anti-inflammatory evaluation. *J. Mol. Struct.,* **1105**: 308-315.

Byrne JD, Betancourt T and Brannon-Peppas L (2008). Active targeting schemes for nanoparticle systems in cancer therapeutics. *Adv. Drug Deliv. Rev.,* **60**(15): 1615-1626.

Cavalli R, Trotta F and Tumiatti W (2006). Cyclodextrin-based nanosponges for drug delivery. *J. Incl. Phenom. Macrocycl. Chem.*, **56**(1-2): 209-213.

Clark M, Jepson M and Hirst B (2001). Exploiting M cells for drug and vaccine delivery. *Adv. Drug Deliv. Rev.*, **50**: 81-106.

Cutrignelli A, Lopedota A, Denora N, Iacobazzi RM, Fanizza E, Laquintana V and Perrone M *et al*. (2014). A new complex of curcumin with sulfobutylether-β-cyclodextrin: characterization studies and *in vitro* evaluation of cytotoxic and antioxidant activity on HepG-2 Cells. *J. Pharm. Sci.,* **103**(12): 3932-3940.

Darandale SS and Vavia PR (2013). Cyclodextrin-based nanosponges of curcumin: formulation and physicochemical characterization. *J. Incl. Phenom. Macrocycl. Chem.*, **75**(3-4): 315-322.

Dash S, Murthy PN, Nath L and Chowdhury P (2010). Kinetic modeling on drug release from controlled drug delivery systems. *Acta Pol. Pharm.,* **67**(3): 217-223.

Dora CP, Trotta F, Kushwah V, Devasari N, Singh C, Suresh S and Jain S (2016). Potential of erlotinib cyclodextrin nanosponge complex to enhance solubility, dissolution rate, *in vitro* cytotoxicity and oral bioavailability. *Carbohydr. Polym.,* **137**: 339-349.

Ferreira F da R, Valentim IB, Ramones ELC, Trevisan MTS, Olea-Azar C, Perez-Cruz F and de Abreu FC *et al*. (2013). Antioxidant activity of the mangiferin inclusion complex with β-cyclodextrin, *LWT - Food Science and Technology,* **51**(1): 129-134.

Florence AT (1997). The oral absorption of micro- and nanoparticulates: Neither exceptional nor unusual. *Pharmaceutical Research,* **14**(3): 259-266.

González-Sarrías A, García-Villalba R, Núñez-Sánchez MÁ, Tomé-Carneiro J, Zafrilla P, Mulero J and Tomás-Barberán FA *et al*. (2015). Identifying the limits for ellagic acid bioavailability: A crossover pharmacokinetic study in healthy volunteers after consumption of pomegranate extracts, *J. Funct. Foods*, **19**: 225-235.

Kobayashi K, Wei J, Iida R, Ijiro K and Niikura K (2014). Surface engineering of nanoparticles for therapeutic applications. *Polymer Journal,* **46**(8): 460-468.

Labrude P and Becq C (2003). [Pharmacist and chemist Henri Braconnot], Revue d'histoire de La Pharmacie, **51**(337): 61-78.

Lei F, Xing DM, Xiang L, Zhao YN, Wang W, Zhang LJ and Du LJ (2003). Pharmacokinetic study of ellagic acid in rat after oral administration of pomegranate leaf extract. *J. Chromatogr. B.,* **796**(1): 189-194.

Lopes MA, Abrahim BA, Cabral LM, Rodrigues CR, Seiça RMF, de Baptista Veiga FJ and Ribeiro AJ (2014). Intestinal absorption of insulin nanoparticles: Contribution of M cells. Nanomedicine: *Nanotechnology Biology and Medicine,* **10**(6): 1139-1151.

Lu J and Yuan Q (2008). A new method for ellagic acid production from Pomegranate husk. *J. Food Process Eng.,* **31**(4): 443-454.

Mady FM and Shaker MA (2017). Enhanced anticancer activity and oral bioavailability of ellagic acid through encapsulation in biodegradable polymeric nanoparticles. *Int. J. Nanomedicine*, **12**: 7405-7417.

Mohanty C and Sahoo SK (2010). The *in vitro* stability and *in vivo* pharmacokinetics of curcumin prepared as an aqueous nanoparticulate formulation, *Biomaterials*, **31**(25): 6597-6611.

Nawwar MAM, Hussein SAM and Merfort I (1994). NMR spectral analysis of polyphenols from *Punica granatum*. *Phytochemistry,* **36**(3): 793-798.

Puică NM, Pui A and Florescu M (2006). FTIR Spectroscopy for the analysis of vegetable tanned ancient leather. *Eur. J. Sci. Theol.,* **2**(4): 49-53.

Seeram NP, Lee R and Heber D (2004). Bioavailability of ellagic acid in human plasma after consumption of ellagitannins from pomegranate (*Punica granatum* L.) juice. *Clinica Chimica Acta,* **348**(1-2): 63-68.

Sharma G, Sonaje K, Italia JL, Tikoo K and Ravi Kumar MN (2007). Biodegradable in situ gelling system for subcutaneous administration of ellagic acid and ellagic acid loaded nanoparticles: Evaluation of their antioxidant potential against cyclosporine induced nephrotoxicity in rats. *J Control Release,* **118**: 27-37.

Shende P, Kulkarni YA, Gaud RS, Deshmukh K, Cavalli R, Trotta F and Caldera F (2015). Acute and Repeated Dose Toxicity Studies of Different β-Cyclodextrin-Based Nanosponge Formulations. *J. Pharm. Sci,* **104**(5): 1856-1863.

Swaminathan S, Cavalli R, Trotta F, Ferruti P, Ranucci E, Gerges I and Manfredi A *et al*. (2010). *In vitro* release modulation and conformational stabilization of a model protein using swellable polyamidoamine nanosponges of β-cyclodextrin. *J. Incl. Phenom. Macrocycl. Chem.,* **68**(1-2): 183-191.

Swaminathan S, Pastero L, Serpe L, Trotta F, Vavia P, Aquilano D and Trotta M *et al*. (2010). Cyclodextrin-based nanosponges encapsulating camptothecin: Physicochemical characterization, stability and cytotoxicity. *Eur. J. Pharm. Biopharm.,* **74**(2): 193-201.

Swaminathan S, Vavia PR, Trotta F and Torne S (2007). Formulation of betacyclodextrin based nanosponges of itraconazole. *J. Incl. Phenom. Macrocycl. Chem.,,* **57**(1-4): 89-94.

Torne SJ, Ansari KA, Vavia PR, Trotta F and Cavalli R (2010). Enhanced oral paclitaxel bioavailability after administration of paclitaxel-loaded nanosponges. *Drug Deliv.,* **17**(6): 419–425.

Vattem DA and Shetty K (2005). Biological functionality of ellagic acid: A review. *J. Food Biochem.,* **29**(3): 234-266.

Zhang HM, Zhao L, Li H, Xu H, Chen WW and Tao L (2014). Research progress on the anticarcinogenic actions and mechanisms of ellagic acid. *Cancer Biology & Medicine,* **11**(2): 92-100.